Self-organized ruptures in an elastic medium: a possible model for earthquakes

1992 J. Phys. A: Math. Gen. 25 L1251

(http://iopscience.iop.org/0305-4470/25/22/005)

J. Phys. A: Math. Gen. 25 (1992) L1251–L1256. Printed in the UK

LETTER TO THE EDITOR

Self-organized ruptures in an elastic medium: a possible model for earthquakes

Huang-Jian Xu†||, Birger Bergersen†, and Kan Chen‡¶

† Department of Physics, University of British Columbia, Vancouver, BC V6T1Z1, Canada

‡ Department of Physics, Simon Fraser University, Burnaby, BC V5A 1S6, Canada

Received 10 August 1992

Abstract. We propose a new discretization scheme for the elastic stress field. Local ruptures give rise to a stress redistribution which can be represented by double couples. The model is applied to earthquake simulation. Computational efficiency is achieved by the use of lattice Green functions. The model allows inclusion of phenomenological features such as annealing and static fatigue.

The aim of this letter is to introduce a new computational approach to the study of fractures in elastic media. For a review of existing methods, see [1]. Most commonly, a local rupture consists of the breaking of a bond (or beam), while we here will consider the breaking of plaquets. In our approach the stress and strain tensors are defined directly on each plaquet, which is our basic unit of discretization. This provides a very efficient algorithm when combined with the use of lattice Green functions.

The method is illustrated by applying it to earthquake simulations. The dynamics of earthquakes is rich and complex [2]. In order to better understand the phenomenology, some essential physics should be included in the models [3]. The tensor character of the stresses needs to be taken into account in a context where the stress redistribution following local ruptures is consistent with elastic theory. Also, a useful model should be able to incorporate some basic properties of rocks (e.g. static fatigue) [2, 4] in the local dynamics.

Our approach is based in part on the crack-propagation model proposed by Chen *et al* [5]. In their model, a rupture occurs when the local stress exceeds a threshold. In addition, a long-range redistribution of force is introduced following a local rupture. This model differs from the more frequently used Burridge–Knopoff model [6, 7] in that it describes an active region rather than a single linear fault. There are shortcomings in the model of [5]. First, the tensorial elastic force is not correctly represented. Second, the model does not exhibit aftershock sequences. The model we describe below overcomes these shortcomings.

|| Present address: Institute of Geophysics and Planetary Physics, University of California, Los Angeles, CA 90024, USA.

¶ Permanent address: Department of Physics, National University of Singapore, Singapore 0511.

0305-4470/92/221251+06$07.50

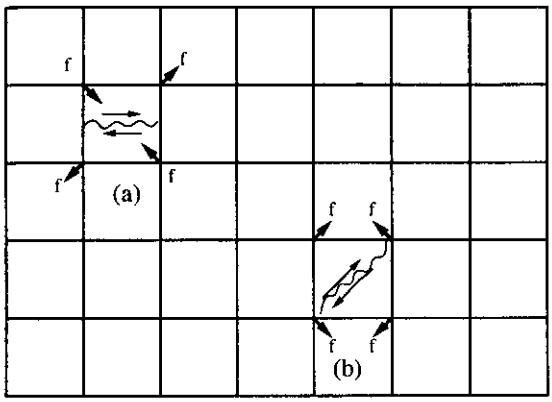

Figure 1. Schematic illustration of a region subjected to external shear stress. The system is divided into many plaquets, and is driven by slowly increasing sheer stress. When a local stress is larger than the corresponding threshold stress, the plaquet fractures, causing a long-range redistribution of elastic forces. The force distribution of local double-couple sources are also illustrated: (a) Fracture in $\hat{e}_x$ direction; (b) Fracture in $\hat{e}_x + \hat{e}_y$ direction.

Our model is illustrated in figure 1. We are focusing on the entire (potential) earthquake region rather than on individual pre-existing faults. For simplicity we only employ a two-dimensional model. Generalization to three dimensions is straightforward. The system is divided into $L \times L$ plaquets. We define a displacement vector $\boldsymbol{u}$ on each node (corner of a plaquet). The distortion of a plaquet is characterized by the strain tensor (defined at the centre of each plaquet)

$$u_{xx}\left(\boldsymbol{r} + \frac{\hat{e}_x + \hat{e}_y}{2}\right) = \frac{1}{2}[u_x(\boldsymbol{r} + \hat{e}_x) - u_x(\boldsymbol{r}) + u_x(\boldsymbol{r} + \hat{e}_x + \hat{e}_y) - u_x(\boldsymbol{r} + \hat{e}_y)] \tag{1}$$

where $\hat{e}_{x,y}$ are unit vectors (the lattice spacing is taken to be unity); u_{yy}, u_{xy} can be expressed similarly. At the beginning, all deformations are elastic, and the stress tensor is related to the strain tensor through the generalized Hooke's law

$$\sigma_{ij}(\boldsymbol{r}) = K u_{ll}(\boldsymbol{r})\delta_{ij} + 2\mu(u_{ij}(\boldsymbol{r}) - \tfrac{1}{3}\delta_{ij}u_{ll}(\boldsymbol{r})) \tag{2}$$

where K, μ are bulk and shear moduli respectively. Before any ruptures occur, the force in the system must be in balance. To be specific, the force components at any node $\boldsymbol{r}$, $F_i = \partial\sigma_{ik}/\partial x_k$ must be zero. The discretized version of F_x is

$$\begin{aligned} F_x(\boldsymbol{r}) = \tfrac{1}{2}[&\sigma_{xx}(\boldsymbol{r} + \boldsymbol{b}) + \sigma_{xx}(\boldsymbol{r} + \boldsymbol{d}) - \sigma_{xx}(\boldsymbol{r} - \boldsymbol{b}) - \sigma_{xx}(\boldsymbol{r} - \boldsymbol{d}) \\ &+ \sigma_{xy}(\boldsymbol{r} + \boldsymbol{b}) + \sigma_{xy}(\boldsymbol{r} - \boldsymbol{d}) - \sigma_{xy}(\boldsymbol{r} - \boldsymbol{b}) - \sigma_{xy}(\boldsymbol{r} + \boldsymbol{d})] \end{aligned} \tag{3}$$

where $\boldsymbol{d} = (\hat{e}_x - \hat{e}_y)/2$ and $\boldsymbol{b} = (\hat{e}_x + \hat{e}_y)/2$. A similar expression can be written for $F_y(\boldsymbol{r})$.

The system is driven by uniformly increasing the shear stress at a constant rate p and we only consider the shear mode of rupture. In the present letter we load the component σ_{xy}. We begin by considering the model without static fatigue. When the stress somewhere exceeds a critical value, it is released while the medium undergoes a local rupture. It is well known that a shear rupture can be modelled by a double-couple (quadrupole) force redistribution [8]. This is due to the fact that no additional force or torque can be generated following a local rupture. The redistribution takes place with the speed of sound. At the positions with increased stress, the stress may now exceed the critical value causing further ruptures; thus the local instability may

cause a chain reaction. Our model does not describe the details of the dynamical process of ruptures (we treat the velocity of sound as infinitely large), but only the stress distribution before and after the rupture. For simplicity we assume that local shear fractures occur only in specific directions, i.e. in the directions of $\hat{e}_x$, $\hat{e}_y$, $\hat{b}$, and $\hat{d}$. We embed the active region which we will simulate in an infinite medium. For our finite system this corresponds to open boundary condition with the activity outside the system neglected. The continuous transfer of stress to the outside region allows a self-organized steady state [9] to develop in spite of the continued loading. Note that the periodic boundary condition will fail completely, because stress cannot be released and the total stress is ever increasing in the system. Let us consider the effect of a local rupture, say a shear fracture in the $\hat{e}_x$ direction at plaquet r_0. After the break the original shear stress at the ruptured site is reduced. The additional stress elsewhere is generated by a double-couple source located at the ruptured plaquet. This leads to a transfer of stress out of the active region (open boundary conditions) allowing a steady state to develop in spite of the continuing increase in stress in this region. In our model the double-couple force distribution is simply four forces acting on the corner nodes of the ruptured plaquet (see plaquet (a) in figure 1)

$$F_d(r) = f\sqrt{2}[b\delta_{r,r_0+b} - d\delta_{r,r_0+d} - b\delta_{r,r_0-b} + d\delta_{r,r_0-d}]. \tag{4}$$

Equation (4) satisfies the requirement that the net force and the net torque generated by the double couple must be zero, and we find the same double-couple force distribution if the rupture is along $\hat{e}_y$. The distribution with respect to fracture in the $\hat{b}$ or $\hat{d}$ direction is shown in plaquet (b) of figure 1. Because we consider special fracture directions, only two components of the stress tensor are needed: $\sigma_1 \equiv \sigma_{xy}$ for determining the condition for fracture in the $\hat{e}_x$ or $\hat{e}_y$ direction and $\sigma_2 \equiv \frac{1}{2}(\sigma_{yy} - \sigma_{xx})$ for determining the condition for fracture in the $\hat{b}$ or $\hat{d}$ direction. In what follows we assume that σ stands for one of these components. The new stress distribution can then be calculated as $\sigma_{new} = \sigma_{old} + \sigma'$, where the elastic contribution to the additional stress σ' is induced by the double-couple source. The non-elastic contribution is only non-zero for the stress component parallel to the fractured surface at the ruptured site. From the force balance condition at the ruptured site we can see that this non-elastic contribution is $-\sqrt{2}f$, an amount that exactly balances the fictitious double-couple forces. For the case where the rupture is in the $\hat{e}_x$ or $\hat{e}_y$ direction, σ_1' and σ_2' are given below

$$\sigma_{1,2}'(r) = -\tilde{f}G_{1,2}(r - r_0) \tag{5}$$

where $\tilde{f} = f\sqrt{2}(K + \mu/3)/(K + 4\mu/3)$ and $G_{1,2}$ are lattice Green functions

$$G_1(r) = \int_{-\pi}^{\pi} \frac{dk_x}{2\pi} \int_{-\pi}^{\pi} \frac{dk_y}{2\pi} \frac{\sin^2 k_x \sin^2 k_y}{(1 - \cos k_x \cos k_y)^2} e^{ik\cdot r} \tag{6}$$

$$G_2(r) = \int_{-\pi}^{\pi} \frac{dk_x}{2\pi} \int_{-\pi}^{\pi} \frac{dk_y}{2\pi} \frac{\sin k_x \sin k_y (\cos k_x - \cos k_y)}{(1 - \cos k_x \cos k_y)^2} e^{ik\cdot r}. \tag{7}$$

The derivation of (4)–(7) is presented in detail elsewhere. We have checked that the Green functions reduce to the correct continuum limit for the double-couple stress

redistribution, and we have obtained excellent agreement with analytical results in a special case [10]. At long distances the Green functions decay as $1/r^d$, where d is the spatial dimension. At short distances the largest stress increase is near the edge of a crack. After the rupture, the shear stress σ_1 ($\equiv \sigma_{xy}$) on the fractured segment is reduced to a percentage x of the original value (in the calculation presented here we use $x = 50\%$, and we have checked that the scaling behaviour is insensitive to x). We have $\sigma_0 + \sigma_1'(r_0) = x\sigma_0$ where σ_0 is the original shear stress just before the rupture. This leads to $-\bar{f}G_1(0) + (1-x)\sigma_0 = 0$, and σ_1', σ_2' can be written as

$$\sigma_{1,2}'(r) = -(1-x)\sigma_0 G_{1,2}(r - r_0)/G_1(0). \tag{8}$$

Similarly, we can obtain the additional stress $\sigma_{1,2}'$ due to a rupture in the direction of $\hat{b}$ or $\hat{d}$

$$\sigma_1'(r) = -(1-x)\sigma_0 G_2(r - r_0)/(1 - G_1(0)) \tag{9}$$

$$\sigma_2'(r) = -(1-x)\sigma_0(\delta_{r,0} - G_1(r - r_0))/(1 - G_1(0)). \tag{10}$$

Again, σ_0 is the original shear stress $\sigma_2(\equiv \frac{1}{2}(\sigma_{yy} - \sigma_{xx}))$ at the ruptured site just before the rupture. Note that the updating of the stress redistribution will be fast since the Green functions only need to be calculated once at the beginning of the simulation.

After each rupture the fractured plaquet is weakened: the stress threshold is reduced to a lower value θ_l (Initially we assign the critical stresses to be random numbers between θ_l and θ). This weakening of fractured surfaces is responsible for generating a fault zone [10]. After the rupture, the fractured surface is allowed to anneal slowly. The annealing process is not well understood. In this letter, we simply assume the strength of the fractured surface will grow as $\theta_i = \theta - (\theta - \theta_l)e^{-(t-t_i)/t_0}$, where t_0 sets the time scale for annealing and t_i denotes the time of the last fracture ($\theta_i(t = t_i) = \theta_l$ by definition). Other annealing laws can also be employed [10]. We have found that the statistical properties discussed in the present letter are insensitive to the annealing law.

We can measure the size of an earthquake by the 'seismic moment' s which is proportional to the total number of sites that have ruptured following the initial instability. We have calculated the distribution of seismic moment and found that it is a power law $N(s) \propto 1/s^\tau$. This is the well known Gutenberg–Richter law [11]. We found the exponent τ to be approximately 1.3, which agrees with the exponent found in [5] within computational errors.

The model which we have described so far, has only two time scales: the slow geological time scale which determines the accumulation of shear stress and the annealing rate. Both time scales are very large. In a real earthquake sequence, however, there appears to be a third and smaller time scale. Although the main shock lasts only for about a minute, the entire earthquake sequence combining foreshocks, mainshock, and aftershocks can last for many weeks. The aftershock sequences are found to obey Omori's law [12]: the rate of aftershocks following the main shock decays as $1/t^\xi$ as a function of time, with the exponent ξ close to one. The most popular explanation of Omori's law is static fatigue [4, 13] that the rock strength is time-dependent. When the applied stress σ is below the instantaneous breaking strength but is above the stress-corrosion limit θ_0, rocks generally break with probability per unit time proportional to $e^{\alpha\sigma}$, where α is a constant.

To illustrate this general physical picture and to verify that our model can be made to satisfy Omori's law, we have modified our model to incorporate the physics of static fatigue. Consider a specific plaquet at the position r_0 in our model. If the shear stress $\sigma_i(r_0)$ is above the instantaneous breaking threshold of the plaquet $\theta_i(r_0)$, the plaquet will fracture as described above. However, when the stress is below θ_i but is still above θ_0, the plaquet is set to break with probability per unit time given by $e^{\alpha(\sigma_i-\theta_i)}$.

Now an earthquake sequence can be defined as follows. When all local stresses are below the respective instantaneous breaking thresholds as well as the stress corrosion limit θ_0, nothing will happen; this is in the period between earthquake sequences, which we call the rest state. Whenever there is a place where the stress is above the local instantaneous breaking threshold or the stress corrosion limit θ_0, ruptures in the systems are expected, and an earthquake sequence begins. The return of the system to the rest state signals the end of this earthquake sequence. Each earthquake sequence can contain many shocks, separated by periods of no activity with some sites still remaining to be fractured by static fatigue. The largest shock in a sequence is defined to be the main shock; the shocks before the main shock are foreshocks and the shocks after it are aftershocks. To check Omori's law, we calculate the number of aftershocks following the main shock as a function of time, and average over many earthquake sequences.

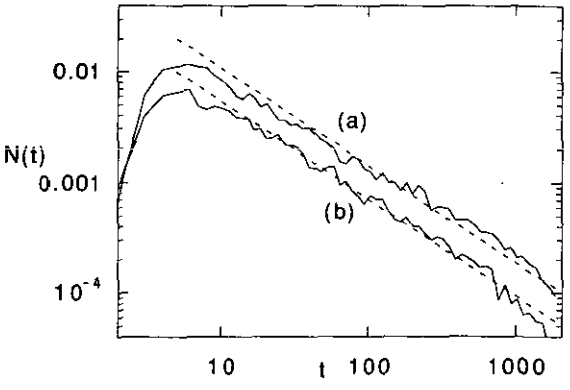

Figure 2. Omori's law: the log–log plots of the rate of (a) aftershock; (b) foreshock as functions of time following (preceding) the mainshock. The parameter values used are defined in the text.

The result of a computer simulation is plotted in figure 2. In the simulation presented we start with zero initial stress and yield strengths randomly distributed between $\theta_l = 0.25$ and $\theta = 1$. Open boundary conditions are employed as described earlier for a 40 × 40 system. The shear stress σ_1 is uniformly increased at the rate $p = 10^{-6}$ until breakages occur, and the stress redistribution following each breakage is computed from (8). The stress corrosion limit σ_0 is taken to be 0.5, and the stress reduction $x = 0.5$. The rate α in the static fatigue law was chosen as 15, while the fault healing time constant t_0 was $0.01/p$. The first 5000 sequences were discarded to allow the system to reach a steady state. The data from the next 5000 sequences is presented in figure 2. Results from a larger system (100 × 100) are in qualitative agreement with the (40 × 40) results. The linearity of the log–log plot indicates the Omori law $N(t) = A/t^{\xi}$ with $\xi \approx 0.90$. We have made a number of runs with modified parameter values, but have not detected any dependence of the exponent on these values. The corresponding result for foreshocks is also plotted. Scholz [14]

found that $\xi = 1$ can be obtained by assuming randomly distributed stress levels induced by the mainshock; this can be viewed as a mean field result in which the spatial correlations are neglected. Simulations with different parameter values and a disscusion of spatial patterns of earthquakes is presented elsewhere [10].

We wish to thank Per Bak and Chao Tang for discussions. This work is supported by the Natural Sciences and Engineering Research Council of Canada.

References

[1] Herrmann H J and Roux S (ed) 1990 *Statistical Models for the Fracture of Disordered Media* (Amsterdam: North-Holland)
[2] Scholz C H 1990 *The Mechanics of Earthquakes and Faulting* (Cambridge: Cambridge University Press)
[3] Knopoff L 1990 *Disorder and Fracture* ed J C Charmet (New York: Plenum) p 279
[4] Atkinson B K 1984 *J. Geophys. Res.* **89** 4077
[5] Chen K, Bak P and Obukhov S P 1991 *Phys. Rev.* A **43** 625
[6] Burridge R and Knopoff L 1967 *Bull. Seismol. Soc. Am.* **57** 341
[7] Carlson J M, Langer J S, Shaw B E and Tang C 1991 *Phys. Rev.* A **44** 884
[8] Burridge R and Knopoff L 1964 *Bull. Seismol. Soc. Am.* **54** 1875
[9] Bak P, Tang C and Wiesenfeld K 1987 *Phys. Rev. Lett.* **59** 381
[10] Xu H-J, Bergersen B and Chen K *Preprint*
[11] Gutenberg B and Richter C F 1956 *Ann. di Geofis.* **9** 1
[12] Omori F 1894 *J. Coll. Sci. Imper. Univ. Tokyo* **7** 111
[13] Scholz C H 1972 *J. Geophys. Res.* **77** 2104
[14] Scholz C H 1968 *Bull. Seismol. Soc. Am.* **58** 1117